5-2015

Ectodomain Mutations Alter the Proteolysis of the Amyloid-β Precursor Protein (APP)

Michael S. Mitsumori
Dominican University of California

https://doi.org/10.33015/dominican.edu/2015.bio.06

Ectodomain Mutations Alter the Proteolysis of the Amyloid-β Precursor Protein (APP)

A thesis submitted to the faculty of

Dominican University of California

And the Buck Institute for Research on Aging

Master of Science

In

Biology

By

Michael Mitsumori

San Rafael, California

May, 2015

Certification of Approval

I certify that I have read *Ectodomain Mutations Alter the Proteolysis of the Amyloidβ Precursor Protein* by Michael Mitsumori, and I approved this thesis to be submitted in partial fulfillment of the requirements for the degree: Master of Sciences in Biology at Dominican University of California and the Buck Institute for Research on Aging.

Varghese John

Graduate Research Advisor

Ph. D.

Clare Libeu

Graduate Research Advisor

Ph. D.

Maria Carranza

Ph. D.

Maggie Louie

Ph. D.

Table of Contents

Abbreviations

AD= Alzheimer's disease

Aβ= Amyloid-β

APP= Amyloid-β Precursor Protein

LOAD= Late-Onset Alzheimer's Disease

SAXS= Small Angle X-Ray Scattering

ADDN= Alzheimer's Disease Discovery Network

Abstract

Alzheimer's disease (AD) is the most common form of dementia, affecting over 5 million Americans. In AD patients there is a buildup of amyloid plaque in the brain, which contributes to AD symptoms. The main component of plaques is Amyloid-β (Aβ), a 40-42 length peptide formed from Amyloid-β Precursor Protein (APP) proteolysis. APP proteolysis can result in either anti-trophic or trophic peptides. Several APP polymorphisms exist that cause or protect against AD by altering APP proteolysis. Recently, more polymorphisms in the APP ectodomain have been discovered in patients with late onset AD (LOAD). The proteolysis of APP may be affected by these mutations, and we aim to determine their effect by measuring the levels of trophic and anti-trophic peptides produced in protein assays, Chinese Hamster Ovary (CHO) cells, and Human Embryonic Kidney (HEK) cells. We discovered that the N585Y APP polymorphism is likely to cause onset of LOAD through increased levels of anti-trophic peptides and decreased levels of trophic peptides.

Acknowledgements

I would like to acknowledge my thesis advisors Dr. Clare Peters-Libeu and Dr. Varghese John for their advice and guidance in the research described in this thesis. I would also like to acknowledge the members of the Bredesen Laboratory at the Buck Institute for Research on Aging, especially Karen Poksay and Jesus Campagna, for their help in the lab. I want to thank Dr. Maria Carranza and Dr. Maggie Louie for their assistance in writing and revising this thesis. Finally, I would like to thank my mother, father, and sisters for all their support.

Specific Aims

Alternative APP proteolysis results in the generation of small peptides that produce either an anti-trophic or trophic effect. Peptides responsible for the anti-trophic effect (Aβ, sAPPβ, APPneo, Jcasp, and C31) play a role in the onset of AD, while trophic peptides (sAPPα, αCTF, p3, and AICD) protect against AD. Mutations to the APP ectodomain may affect its proteolysis by BACE and ADAM10, resulting in altered formation of anti-trophic and trophic peptides. Our proposed study aims to determine if this phenomenon occurs *in vitro*. We will investigate by conducting the following specific aims:

(1) Creating APP ectodomain mutants.

(2) Purifying mutant protein and conducting cleavage assays to measure the effect of mutations on proteolytic cleavage.

(3) Expressing mutants in Chinese Hamster Ovary Cells (CHO) and Human Embryonic Kidney Cells (HEK) and detecting cleavage products to determine the *in vitro* effect of mutations on proteolytic cleavage.

Introduction

I. Impact

Alzheimer's disease (AD) has an enormous effect on communities, families, the health care system, and the individuals diagnosed with the disease. In 2014, an estimated 5.2 million Americans had AD, of which 5 million were over the age of 65 (1). One in nine people over the age of 65 has AD, and one-third of people older than 85 have AD (2). Every 67 seconds, someone develops a new case (2). The number of deaths from AD was 84,767 people in 2013, making AD the 6th leading cause of death in the United States (3). Total cost of AD care in 2015 was estimated at $226 billion, with Medicare and Medicaid covering around $153 billion. Out-of-pocket spending will account for $44 billion (2).

The number of AD patients is expected to increase in the future as the segment of the US population over the age of 65 increases (4). In 2010, thirteen percent of the population was over the age of 65 (5). Estimates show that by 2030, twenty percent of the population will be over the age of 65 (5). By 2025, the number of AD patients will have increased to 7.1 million (1). By mid-century, a projected 13.8 million people will have AD (1), with a new case arising every 33 seconds (2).

II. Symptoms and Treatment

AD symptoms vary per person, but commonly begin with a gradual decrease in the ability to remember new information. As AD progresses, affected individuals experience further difficulties such as memory loss that disrupts daily life, challenges in planning or solving

problems, difficulty in completing familiar tasks, confusion with time or place, trouble understanding visual images and spatial relationships, new problems with words in speaking or writing, misplacing things and losing the ability to retrace steps, decreased or poor judgment, withdrawal from work or social activities, and/or changes in mood and personality (primarily apathy and depression). In the late stages of the disease, people require assistance to perform basic activities (bathing, eating, dressing, using the bathroom, etc.), lose the ability to communicate, fail to recognize loved ones, and become bed-bound and reliant upon around-the-clock care. (2)

Although there is no cure for AD, pharmacologic and non-pharmacologic therapies are employed with varied results to treat symptoms. There are dozens of drugs and therapies being researched throughout the world (2). Currently, six drugs have been approved by the U.S. Food and Drug Administration that temporarily improve AD symptoms by increasing the amount of neurotransmitters in the brain (6). The effectiveness of these drugs has varied per person. Non-pharmacologic treatments have largely been ineffective, with the exception of cognitive stimulation (7). More research is required to identify effective pharmacologic or non-pharmacologic therapies or cures.

III. Late-Onset Alzheimer's Disease (LOAD) and Early-Onset Alzheimer's Disease (EOAD)

AD can be divided into two types: Early-Onset Alzheimer's Disease (EOAD) and Late-Onset Alzheimer's Disease (LOAD) (figure 1). EOAD patients consist of 5-10% of the total AD population and are diagnosed with AD before reaching 65 years of age (8, 9). Fifty percent of EOAD cases are familial Alzheimer's disease (FAD), which is caused by mutations in APP, PSEN,

or Tau (10, 11). LOAD patients consist of about 95% of the total AD population and are diagnosed with AD after turning 65 years of age (8, 9, 11). LOAD is primarily caused by environmental factors, but may involve genetic risk factors (8) such as the APOE4 allele or APP ectodomain mutations.

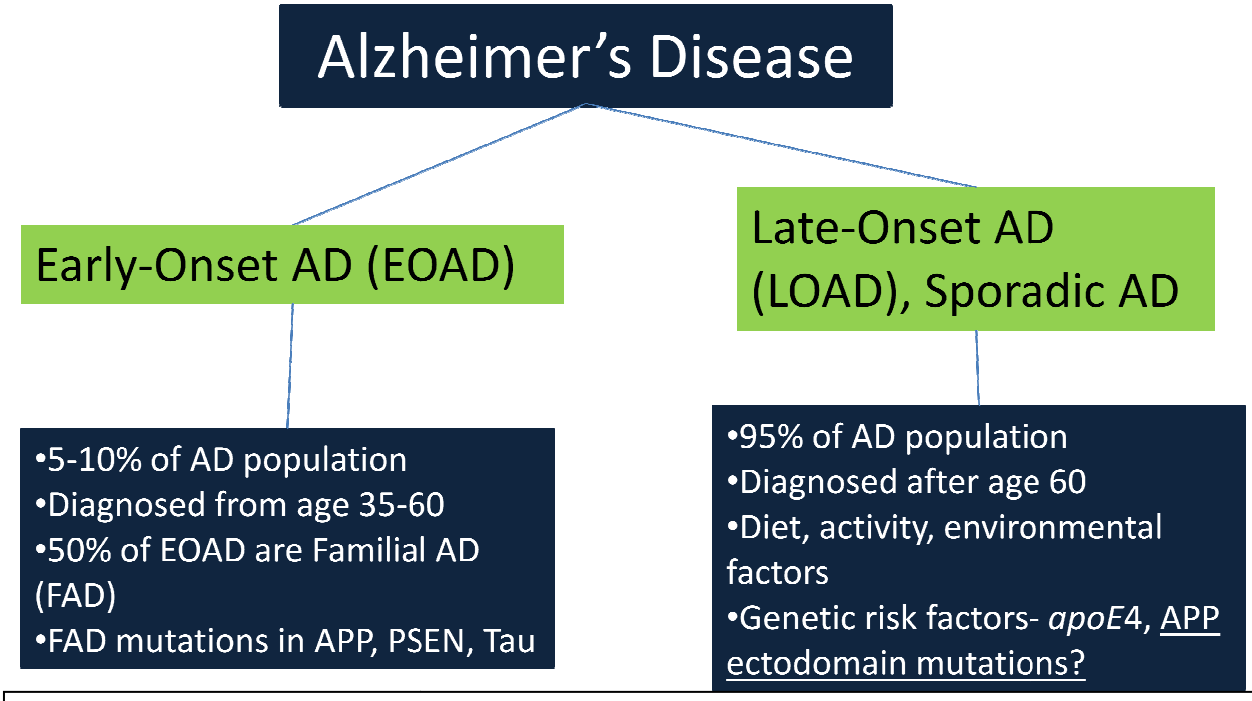

Figure 1. EOAD and LOAD. AD can be divided into two types: Early-Onset Alzheimer's Disease (EOAD) and Late-Onset Alzheimer's Disease (LOAD). The majority of AD patients have LOAD, which occurs after age 65 and is caused by environmental factors or genetic risk factors. Only a small portion of AD patients have EOAD, which occurs before age 65 and is caused by mutations to APP, PSEN, and Tau.

IV. Amyloid Plaques and Neurofibrillary Tangles

The pathological hallmarks of AD include the buildup of amyloid plaque in extracellular space of the brain and the intercellular buildup of neurofibrillary tangles (12) (figure 2).

Amyloid plaques are composed of the Amyloid-β peptide (Aβ), a 40-42 length peptide formed from the proteolytic cleavage of the Amyloid-β Precursor Protein (APP) (13). Aβ plays an important role in the development of AD, and studies have shown that its properties include a detergent-like effect, metal binding (14, 15), activation of cell death pathways (16, 17), interaction with extracellular receptors (18, 19, 20), and generation of reactive oxygen species (21).

In AD, there is also a buildup of neurofibrillary tangles that are composed of hyperphosphorylated Tau proteins. Tau proteins are a part of the microtubule-associated proteins family, and assist with the formation and stabilization of microtubules (22). Tau protein ability to bind microtubules is dependent on its phosphorylation state, which is regulated by kinases and phosphatases (23). When hyperphosphorylated under certain conditions, Tau proteins form oligomers (24) that compose the neurofibrillary tangles observed in AD.

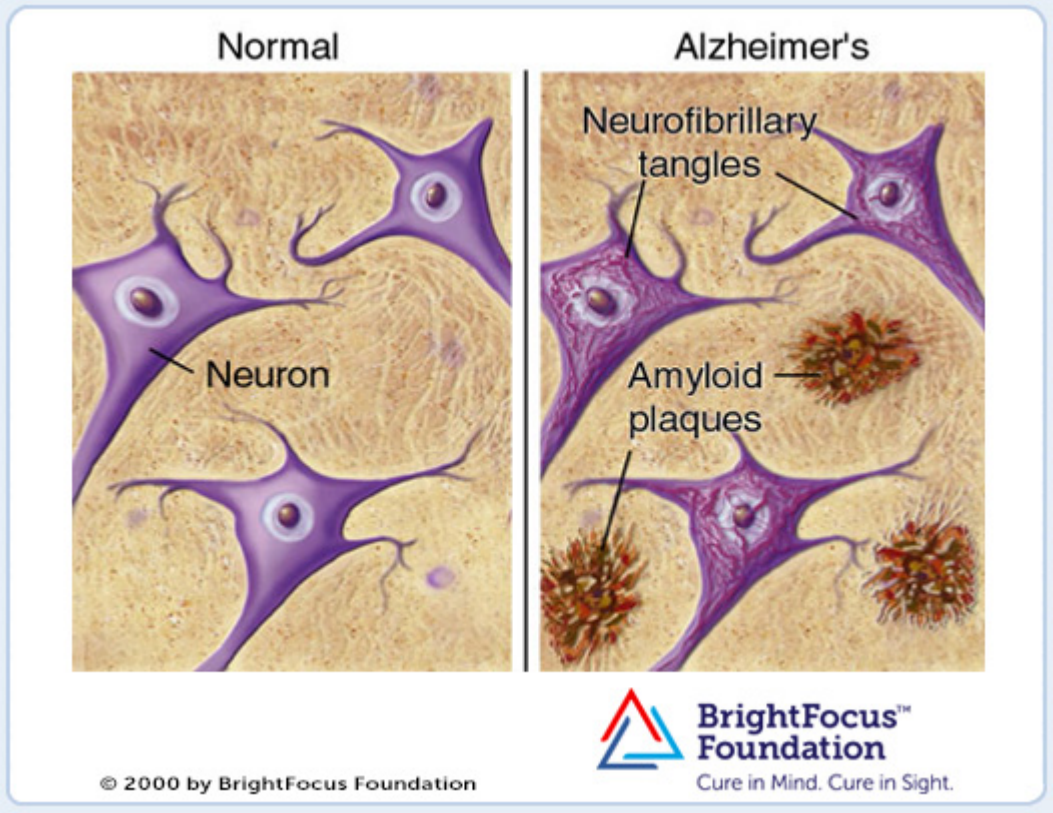

Figure 2. The hallmarks of AD: amyloid plaques and neurofibrillary tangles. Amyloid plaques are composed of Aβ peptides formed through proteolytic cleavage of APP. Neurofibrillary tangles are composed of hyperphosphorylated Tau proteins, which assist with microtubule formation and stabilization.

V. APP Proteolysis- Formation of Trophic and Anti-Trophic Peptides

The formation of the Aβ peptide found in amyloid plaques occurs during the proteolysis of APP. APP proteolysis is an event that occurs when APP, a type I transmembrane protein, is cleaved by several proteolytic enzymes called secretases to produce either trophic or anti-trophic peptides (25, 26) (figure 3). Trophic peptides are amino acid chains that affect the cell by stimulating cell growth, differentiation, and survival (26). Anti-trophic peptides produce the

opposite effect, inhibiting cell growth and differentiation, and activating cell death pathways (26). During anti-trophic peptide formation, β secretase (BACE) and γ-secretase cleave APP at the β and γ-sites, respectively, resulting in the products Aβ and sAPPβ (25, 26, 27). Further intracellular proteolytic processing produces Jcasp and C31. These peptides are involved in the anti-trophic effects that lead to AD (26). Alternatively, APP processing can produce trophic peptides (26). APP is cleaved by α secretase (ADAM10) at the α-cleavage site, resulting in the formation of sAPPα and αCTF, two trophic peptides that protect against AD (26).

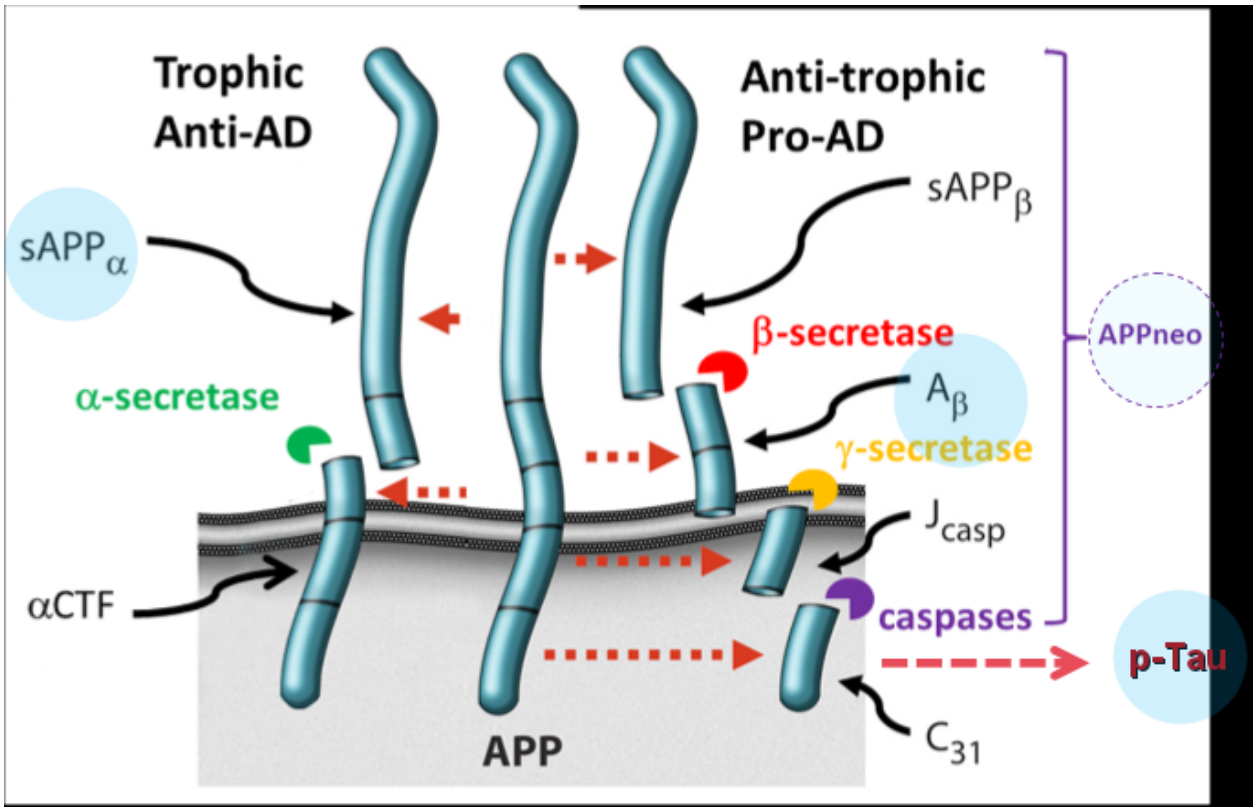

Figure 3. Alternative APP proteolysis. APP cleavage produces either trophic or anti-trophic peptides. When initial cleavage occurs at the β site, anti-trophic peptides are produced. However, if initial cleavage occurs at the α site, trophic peptides are produced.

Several recent studies have demonstrated that alternative APP proteolysis can be altered through interactions with biological molecules other than the proteolytic enzymes (28). In the absence of Aβ, APP exists as a homodimer. Dimeric Aβ induces monomerization of APP, while Aβ oligomers stabilize the APP homodimer (29). APP dimerization can influence APP proteolysis. Small molecules such as disulfiram and sulfiram, which inhibit APP dimerization, enhance the production of sAPPα (30). A group led by Dr. Selkoe measured sAPPα and sAPPβ levels to determine the activity of proteolytic enzymes in the presence of various known APP ligands (31). Using sAPPα and sAPPβ levels to determine proteolytic activity is a useful method, and we will employ this method in determining the effect of APP ectodomain mutations on APP proteolysis. The Bredesen laboratory and other groups have shown that an important interaction occurs between sAPPα and BACE, and the association of these two molecules inhibits Aβ production (32, 33). Furthermore, decreasing sAPPα levels results in an increase of Aβ (32). APP ectodomain mutations may affect the ability of APP to interact with these biological molecules. Study of LOAD mutants may reveal altered interactions that result in altered levels of APP cleavage products and increased or decreased risk of AD.

VI. APP Structure

The APP ectodomain consists of various regions with unique functions (figure 4). The E1 region contains the Growth Factor-like Domain (GFLD) and the Copper Binding Domain (CuBD) and is nearest the N terminus (34). The E2 region contains the RERMS sequence and is capable of binding other proteins (35). The acidic region, composed primarily of acidic residues,

connects the E1 and E2 regions (34). Acidic region function is unknown and no other human protein contains a similar region (36).

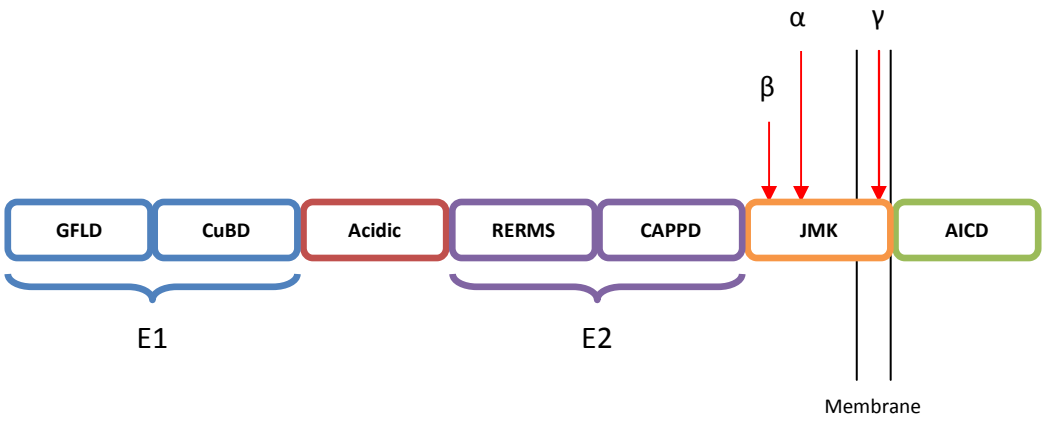

Figure 4. APP structure. Shows the various regions and domains of APP. The E1 region is located nearest the N terminus and consists of the Growth Factor-like Domain (GFLD) and the Copper Binding Domain (CuBD). The E2 region contains the RERMS sequence and the Central APP Domain (CAPPD) and is capable of interaction with other proteins. The acidic region is composed primarily from acidic residues, connects the E1 and E2 regions, and has unknown function. The β, α, and γ sites are areas where APP is cleaved by proteolytic enzymes.

VII. Known APP Mutations

Several polymorphisms have been found to have an effect on APP proteolysis. The Icelandic APP polymorphism was found to be protective against AD. It is located near the β-cleavage site and reduces the amount of anti-trophic peptides produced (39). It is possible that more APP polymorphisms exist that can also protect against AD.

Two other polymorphisms shift APP proteolysis towards the formation of anti-trophic peptides and have been linked with EOAD. The Swedish APP mutation is located near the β-cleavage site and increases the amount of Aβ produced (37). The Indiana APP mutation is located within the APP transmembrane domain near the γ-cleavage site (38). It is possible that more APP polymorphisms exist that shift APP proteolysis towards the formation of anti-trophic peptides that cause or increase risk of AD. In this study, we will investigate several candidate polymorphisms that are likely to alter APP proteolysis.

VIII. APP Ectodomain Mutations

A recent study has discovered several APP ectodomain variants found in late onset AD (LOAD) patients (40) (figure 5). It is unknown how these variants contribute to AD. In order to shed light on their mechanism of action, we chose the N585Y and E191G for detailed study. The E426K and D243N are other candidates for this study. The N585Y variant is located near the β-cleavage site. The E426K variant is located in the E2 region and the E191G and D243N variants are located in the APP acidic region, which has unknown function. Studies of one of these mutants may provide insights towards acidic region function and any effects on APP proteolysis. The table below (figure 5 a.) shows the various mutants, their location within APP, and their previously observed effect. The H147N variant is not associated with LOAD, is located in the CuBD, and was reported to increase intracellular sAPPα levels (41).

a.

Mutation	Location	Observed Effect
N585Y	β-cleavage site	Unknown
E426K	E2 Region	Unknown
E191G	Acidic Region	Unknown
D243N	Acidic Region	Unknown
H147N (non-LOAD)	CuBD	↑ intracellular sAPPα

b.

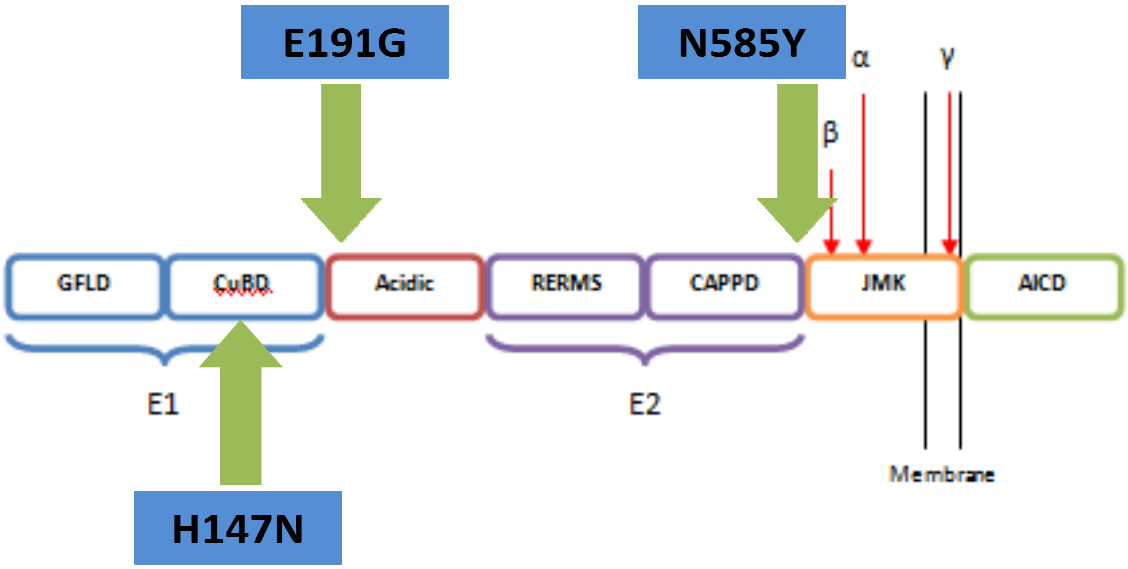

Figure 5 a. Table of the known APP ectodomain mutations, their location, and observed effect. Mutations in bold are the ones involved in this study. **b.** Location of the E191G, N585Y, and H147N are shown on an APP model.

These APP ectodomain mutations can have a wide range of effects. Mutations may affect APP interaction with physiological binding partners, including the proteolytic enzymes responsible for APP proteolysis. Altered interaction with these enzymes would likely affect secreted and intracellular levels of APP cleavage products in CHO cells. Mutations may also

cause conformational changes to cleavage sites, affecting proteolytic activity. These conformational changes would also alter cleavage product levels. Because cleavage product levels are an indication of altered interaction with proteolytic enzymes and can affect the onset of AD, we aim to measure the cleavage products of APP ectodomain mutations. The mutations that we have focused on in this study are the N585Y, the E191G, and the H147N. Because the N585Y is located close to the β-cleavage site, we believe that is the most likely of the mutations to alter cleavage product levels. The E191G mutation is located within the acidic region of APP, and we believe that studying this mutant may provide insights toward the function of that region. The H147N has been the focus of other studies (9), and we aim to use it as a positive control in our experiments.

Research Design and Methods

I. Computer Modeling

To aid in predicting the effect of APP ectodomain mutations on APP cleavage, mutations were mapped on a model of APP. The model created by Dr. Clare Peters-Libeu represents a possible structure of APP based on computer modeling data derived from small angle x-ray scattering (SAXS) data (33). The program Chimera was used to mark the location of the mutants studied.

II. Mutagenesis

To create mutants, pDEST-HisMBP plasmid containing wild type APP695 were used for expression in Rosetta-gami B (RGB) cells (plasmid shown below). For transfection in CHO cells, pcDNA3 plasmids containing mutant or wild-type APP695 were used. Mutations were introduced using the Quikchange II XL Site-Directed Mutagenesis Kit (Agilent Technologies, Santa Clara, CA) using primers designed with the primer design tool at http://www.genomics.agilent.com/primerDesignProgram.jsp?&_requestid=1597773.

Mutagenesis reactions were prepared by adding 5 µL of 10x reaction buffer, 10 ng of pDEST-HisMBP plasmid containing wild-type APP695, 125 ng of primer #1, 125 ng of primer #2, 1 µL of dNTP mix, 3 µL of QuikSolution, and ddH_2O to a final volume of 50 µL to a PCR tube. One µL of *pfuUltra* HF DNA Polymerase was added, and the PCR reaction was cycled according to the QuikChange II XL handbook parameters (shown below).

TABLE I

Cycling Parameters for the QuikChange® II XL Method

Segment	Cycles	Temperature	Time
1	1	95°C	1 minute
2	18	95°C	50 seconds
		60°C	50 seconds
		68°C	1 minute/kb of plasmid length
3	1	68°C	7 minutes

* For example, a 5-kb plasmid requires 5 minutes at 68°C per cycle.

Following PCR cycling, 1 µL of *Dpn* I restriction enzyme was added to each reaction to digest nonmutated DNA, and reactions were incubated at 37°C for 1 hour. DPN I digestion was followed by an XL10-Gold transformation to increase plasmid yield. XL10-Gold ultracompetent cells stored at -80°C were first thawed on ice. Forty-five µL of cells were transferred to

prechilled 14 mL Falcon polypropylene round-bottom tubes and 2 µL of β-ME was added. The cells were incubated on ice for 10 minutes, swirling every 2 minutes. Two µL of *Dpn* I-treated plasmid was then added to the cells. Following a 30 minute incubation on ice, the cells were heat shocked in a 42^{o}C water bath for 30 seconds. The cells were then incubated on ice for 2 minutes and 0.5 mL of SOC, preheated to 42^{o}C, was added. Reaction mixtures were then incubated at 37^{o}C for 1 hour with shaking at 250 RPM. Cells were plated onto NIM plates with carbenicillan and incubated at 37^{o}C overnight. A Qiagen miniprep kit (Qiagen, Hilden, Germany) was used to isolate mutated DNA from the plated cells.

III. RGB Transformation

Once mutant APP695 pDEST-HisMBP plasmids were created, they were transformed into RGB cells for protein expression. RGB is a strain of *E. coli* that is designed to enhance the expression of eukaryotic proteins through its deficiency in *lon* and *ompT* proteases (prevents protein degradation), mutations to thioredoxin reductase (*trxB*) and glutathione reductase (*gor*) (enhances disulfide bond formation in cytoplasm), and addition of specific tRNAs that are rarely used in *E. coli*. RGB cells stored at -80^{o}C were first thawed on ice. Twenty µL was then added to chilled 1.5 mL microcentrifuge tubes and 2 µL of pDEST-HisMBP plasmid containing wild-type or mutant APP695 was added. Tubes were placed on ice for 5 minutes, heat shocked in a 42^{o}C water bath for 30 seconds, and then placed on ice for 2 minutes. Eighty µL of SOC media was added, and tubes were incubated in a shaker set to 250 RPM for 1 hour at 37^{o}C. Finally, RGB cells were plated onto NIM plates with carbenicillan and chloramphenicol and incubated at 30^{o}C for two days.

IV. Expression

Mutant and wild-type APP695 protein was expressed by inoculating 30 mL of NIM media with RGB cells containing mutant APP pDest-HisMBP plasmids and shaking overnight at 280 RPM at 30°C. Using 3 mL of this overnight culture, 1L of LB was inoculated and grown while shaking at 280 RPM at 30°C until OD 600 nm was close to 0.5-0.6. Expression was induced by adding 0.1 mg/mL IPTG and shaking for 10-12 hours at 280 RPM at 24°C. Finally, cultures were moved to 4°C for 10-24 hours.

V. Purification

Mutant protein was purified from RGB cells following transformation and expression steps. Mutant and wild-type APP695 were purified employing the same methods. Samples were lysed, and then purified through the use of nickel beads, dialysis, a heparin column, and a size exclusion column (figure 6). Prior to lysis, RGB cells containing expressed mutant and wild-type APP695 were collected from expression cultures by centrifugation at 6000 RPM at 4°C for 15 minutes and discarding the supernatant.

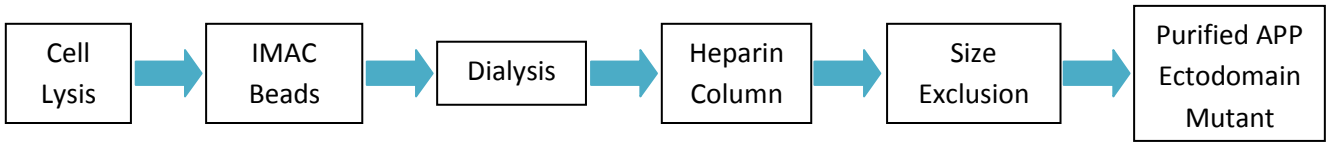

Fig 6. The steps required for purification of APP695 Ectodomain Mutants.

Cell Lysis. RGB Cells containing expressed mutant and wild-type APP695 protein were lysed to release protein. A 20mM Tris pH 6.8, 100mM NaCl, 5mM EDTA, 0.1 mg/mL lysozyme

lysis buffer with Sigma Fast Protease Inhibitor was used for the cell lysis, and all cell lysis steps were completed on ice to prevent protein degradation. The RGB cells were first resuspended in the lysis buffer and then transferred to a tissue homogenizer. After homogenization, samples were centrifuged at 5,000xg at 4^{o}C for 1 hour. The pellet was discarded and the supernatant was collected. Two Fast Protease Inhibitor tablets (Sigma-Aldrich, St. Louis, MO) were added to the supernatant.

IMAC Beads. The protein-containing-supernatant collected during cell lysis step was then applied to IMAC beads (Roche Diagnostics, Indianapolis, IN). IMAC beads contain nickel ions, which purify by binding the His-tag attached to mutant and wild-type APP695. The IMAC beads were first equilibrated using an equilibration buffer of 20 mM Tris pH 7.4, 100 mM NaCl, and 5 mM EDTA. The protein sample was then added to the IMAC beads and placed at 4^{o}C for 4 hours with gentle rocking. Next, the IMAC bead-protein mixture was centrifuged at 3,000xg at 4^{o}C for 10 minutes. The supernatant was removed and the pellet resuspended in equilibration buffer and transferred to a 10 mL centrifuge column. After the flow through was collected, a wash buffer of 20 mM Tris pH 7.4, 250 mM NaCl, 2.5 mM EDTA, a 2 mM imidazole was added. The wash was collected, the columns were closed, and an elution buffer of 20 mM Tris pH 7.4, 100 mM NaCl, 5 mM EDTA, and 100 mM imidazole was added. The beads were resuspended and placed at 4^{o}C for 20 minutes with gentle rocking. Finally, the columns were opened and the elution containing mutant or wild-type APP695 was collected.

Dialysis. Following the IMAC Beads step, the collected elution contained mutant or wild-type APP, other proteins, 20 mM Tris pH 7.4, 100 mM NaCl, 5 mM EDTA, and 100 mM

imidazole. The purpose of the dialysis step is to remove the imidazole from the sample. First, 5L of a 20 mM Tris pH 7.4, 100mM NaCl, and 5 mM EDTA buffer was prepared. The sample was added to a dialysis bag of MWCO 6-8,000. The sample-containing dialysis bag was placed into the 5 L of buffer for 1 hour. The dialysis bag was then removed, and the sample was collected in a 50 mL conical tube.

Heparin Column. Following dialysis, a heparin column was used to further purify mutant and wild-type APP695 from solution. First, the heparin column was cleaned by running water, 10 column volumes of 2M NaCl, 10 column volumes of 200 mM NaOH, 20 column volumes of 20 M tris pH 8, 10 column volumes of 70% ethanol, and 10 column volumes of 20% ethanol 50 mM sodium acetate through it. The column was then equilibrated with 10 column volumes of 20 mM tris pH 7.4, 2.5 mM EDTA. Next, the sample was loaded onto the column, and the flow through was collected. The column was eluted by fraction collection and increasing the concentration of NaCl. The 1st fraction was collected using 50 mL of 20 mM tris pH 7.4, 2.5 mM EDTA, and 0 mM NaCl. The 2nd fraction was collected using 50 mL of 20mM tris pH 7.4, 2.5 mM EDTA, and 100 mM NaCl. The 3rd, 4th and 5th fractions were collected in similar fashion, using 20 mM tris pH 7.4, 2.5 mM EDTA, and 300, 400, or 500 mM NaCl. The fraction containing mutant or wild-type APP695 was determined using a gel and western blot.

Size Exclusion Column. The final purification step for mutant and wild-type APP695 is size exclusion chromatography. The heparin column fraction containing mutant or wild-type APP695 was run through the sizing column. Fractions were collected and a gel and western

blot was used to determine which fraction contained the target protein. Samples were used to conduct AlphaLISA cleavage assays (PerkinElmer, Waltham, MA).

VI. Chinese Hamster Ovary (CHO) Cell Culture

Wild-type CHO cells were used for these experiments as they should not express endogenous APP, which would cause interference. Cells were maintained at 37^{o}C in 5% CO_2 in F-12K media (ATTC, Manassas, VA) supplemented with 10% fetal bovine serum, penicillin, and streptomycin in 10 cm tissue culture dishes. Media was changed every 2 days, and cells were split every 3 days or when confluence reached 70-90%.

VII. Human Embryonic Kidney (HEK) Cell Culture

Wild-type HEK cells were 37^{o}C in 5% CO_2 in DMEM media (Sigma-Aldrich, St. Louis, MO) supplemented with 10% fetal bovine serum, penicillin, and streptomycin in 10 cm tissue culture dishes. Media was changed every 2 days, and cells were split every 3 days or when confluence reached 70-90%.

VIII. Transfection

Wild-type CHO or HEK cells were each transfected with three pcDNA3 plasmids. The first plasmid contains the LacZ gene, and is used for measuring transformation efficiency. The second plasmid contains BACE1, the proteolytic enzyme that cleaves APP at the β-site. The third plasmid contains wild-type or a mutant APP695. Cells were first transferred from 10 cm tissue culture dishes to 24 or 6-well plates. For LacZ, BACE1, and ADAM10 cleavage assays, 24-well plates were used. For western blotting, 6-well plates were used. Cells were grown to 70-

90% confluence in 10 cm tissue culture dishes at 37^{o}C in 5% CO_2. The media was removed, and 3 mL of 0.25% trypsin solution (Corning, Manassas, VA) was added to each tissue culture dish. The cells were then incubated at 37^{o}C in 5% CO_2 for 10 minutes, then transferred to 15 mL conical tubes and centrifuged at 1,500 RPM for 5 minutes at room temperature. The trypsin was then removed, and the cells were resuspended in 4 mL of F-12K media. For plating on 24-well plates, 1 mL of resuspended cells was added to 5 mL of F-12K media, and 500 µL of this mixture were added to each well in a 24-well plate. For plating on 6-well plates, 1 mL of resuspended cells was added to 12 mL of F-12K media (CHO cells) or DMEM (HEK cells), and 2 mL of this mixture were added to each well in a 6-well plate. 24 and 6-well plates were incubated at 37^{o}C in 5% CO_2 until cell confluence reached 70-90%. Cells were then transfected with pcDNA3 plasmids containing LacZ, BACE1, and wild-type or mutant APP695. The media was removed from each well, and 250 µL of fresh media was added to each well in the 24-well plate. One mL of fresh media was added to each well in the 6-well plate. Five µg of each plasmid was added per well, along with 3.5 µL of Lipofectamine per well. Transfected cells were then incubated at 37^{o}C in 5% CO_2. After 4 hours, the media was discarded, and fresh media was added (250 µL for 24-well plates; 1 mL for 6-well plates). Plates were then incubated overnight at 37^{o}C in 5% CO_2.

IX. Lysis

After transfection and overnight incubation, the media and cell lysis were collected. The media was removed from the cells and transferred to a fresh plate. 1 mL of trypsin was added to each well containing transfected cells. Plates were then incubated at 37^{o}C in 5% CO_2 for 5

minutes. The removed media was then place back to its corresponding wells, and the media, cell; trypsin mix was moved to 1.5 mL microcentrifuge tubes. The tubes were spun at 2,000 x g for 10 minutes at 4^{o}C. The supernatant was transferred to new 1.5 mL tubes and protease inhibitors were added. The pellet was resuspended in AlphaLISA HiBlock Buffer with protease inhibitors if LacZ and AlphaLISA assays were to be performed. For western blots, the pellet was resuspended in RIPA buffer with protease inhibitors. Because LacZ and AlphaLISA assays use a different lysis buffer than western blot, a single transfection can result in either LacZ and AlphaLISA assays or a western blot. Separate transfections were done for assays and western blots.

X. Western Blot

Western blot was used to verify the presence of wild-type or mutant APP695 in cell lysate. CHO or HEK cells grown in 6 well plates were transfected and lysed. The lysate was then sonicated for three 5 second pulses at amplitude of 80 nm to degrade DNA. The protein concentration for each sample was determined through a coomassie assay, and 25-50 µg of protein in each sample were added to lanes in a Novex NuPage 4-12% Bis-Tris (Life Technologies, Grand Island, NY) and ran at 200V for 55 minutes in MOPS Buffer. Gels were removed and washed 3 times in water, 10 minutes each wash. GelCode Blue (Life Technologies, Grand Island, NY) was added to the gel for 1 hour, followed by water for 30 minutes. Protein was then transferred to a nitrocellulose membrane. 5% milk in TBST was used for blocking. Primary antibodies used were 3E9, 2B3, anti-sAPPβ, and anti-BACE. Secondary

antibody was anti-mouse for 3E9 and 2B3; anti-rabbit for anti-sAPPβ and anti-BACE. Mutant or wild-type APP695 was detected using ECL detection kit (Thermo Fisher Scientific, Carsbad, CA).

XI. LacZ Assay

LacZ assay was used to determine the effectiveness of cell transfections. Fifty µL of LacZ buffer was added to 50 µL of cell lysate in a LacZ assay plate. Plates were read at 420 nm every 30 minutes for 3 hours.

XII. BACE and ADAM10 AlphaLISA Cleavage Assay

Cell lysate, cell media, and purified mutant or wild-type APP695 were used in AlphaLISA assays. Purified mutant or wild-type APP695 was first added to a well in a 365-well plate with acceptor beads and antibody. BACE or ADAM10 was then added and samples were incubated at room temperature for 60 minutes. Donor beads were added and samples were incubated at room temperature for 30 minutes in darkness. The beads were excited at 530nm, $^{1}O_{2}$ produced upon binding of the beads in proximal location, and the plates were read at 680 nm.

Results

I. Computer Modeling

Mapping results suggest that the N585Y mutation could affect the binding site of APP and BACE1 as N585 is located in the region where BACE interacts with APP (figure 7). Other mutations are located far from the binding site of BACE1 to APP, but could still cause conformational changes that affect BACE1 cleavage. Not affecting BACE1 cleavage does not

mean the mutation does not affect APP proteolysis. It could be possible that these mutations play a role in APP-ADAM10 interaction, or affect endocytosis or secretion of APP or cleavage products.

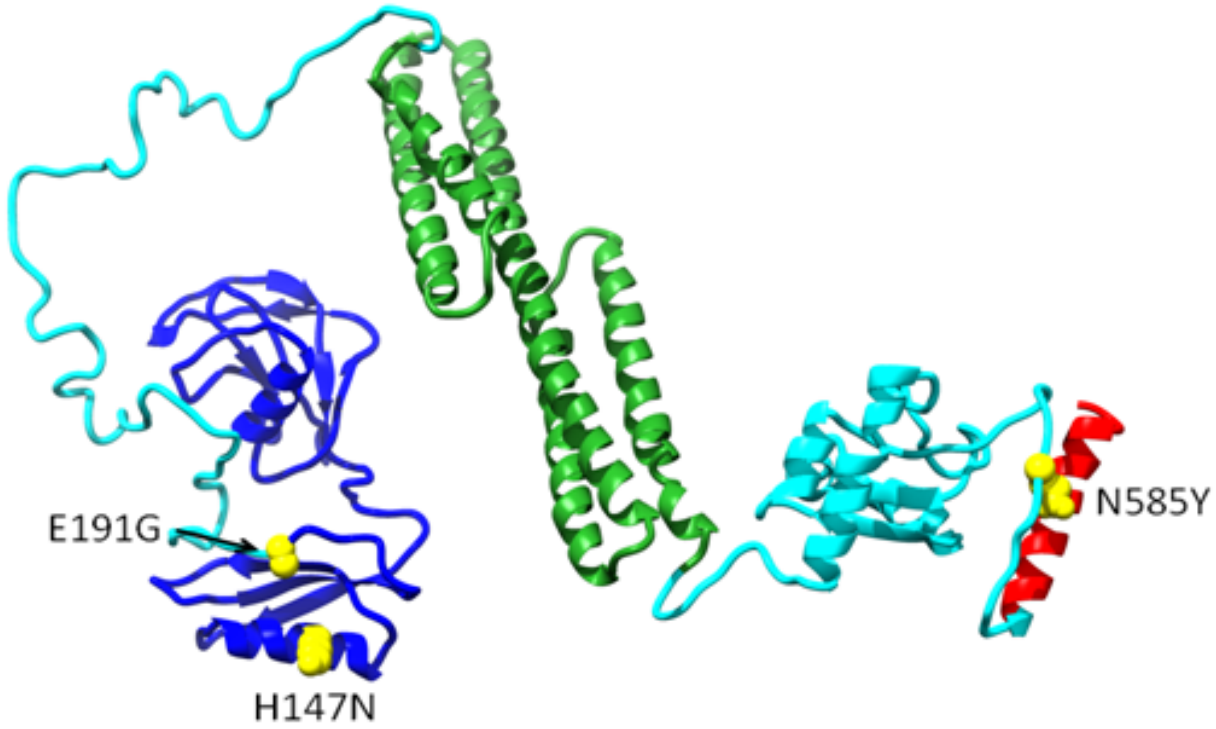

Figure 7. Model showing the domains of APP and known ectodomain mutations involved in this study. The E1 domain is shown in dark blue. The E2 domain is shown in green. The Aβ region is shown in red. The acidic domain and JMK region are shown in cyan. The three mutations N585Y, E191G, and H147N are shown in yellow. The N585Y mutation is located near the β-cleavage site and hence likely to affect BACE1 interaction with APP. The other mutations may affect APP conformation and shape, which could also affect interaction with BACE1 or alter cellular trafficking of APP.

II. Protein Purification

Mutant and wild-type APP695 were purified for BACE assays that would measure protein sensitivity to BACE cleavage. Mutant or wild-type APP695 plasmids were transformed into RGB cells and expression was induced. RGB cells were lysed, and the lysate was applied to IMAC beads, a heparin column, and a sizing column. A gel shows the fully purified H147N and E191G proteins and the N585Y, which has been partially purified (figure 8).

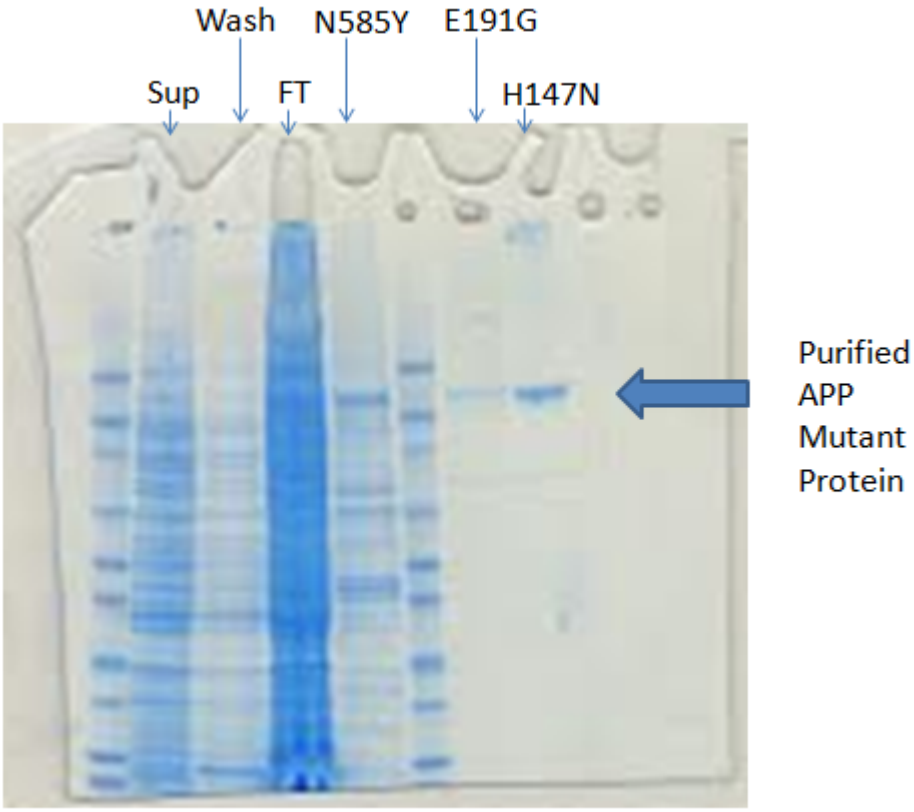

Figure 8. Gel of purified and partially purified mutant APP695. The E191G and H147N have been fully purified and are ready for BACE assay. The N585Y has only been partially purified. The N585Y lysate was applied to the IMAC beads and the supernatant (sup), wash, flowthrough (FT), and elution (N585Y) were collected. The N585Y elution will next be applied to a heparin column.

III. CHO Cells

To determine the effect of mutations on APP cleavage, mutant and wild-type APP was transfected into wild-type CHO cells. Cells were lysed after 48 hour incubation at 37^{o}C in 5% CO_2, and lysis was analyzed using a 4-12% bis-tris gel and western blot. A primary antibody for GAPDH was used to show protein concentration was equal in each well (figure 9). A primary antibody for BACE was used to show the presence of BACE in cells containing BACE pcDNA3 plasmid (figure 9). Primary antibodies for sAPPα and sAPPβ were used to detect the presence of APP cleavage products (figure 9) and primary antibody 3E9 for APP and APP cleavage products was used to detect presence of APP. ELISA assays were used to measure sAPPα and sAPPβ levels in media and cell lysate and the percent change in sAPPβ and sAPPα levels were calculated (figures 10,11).

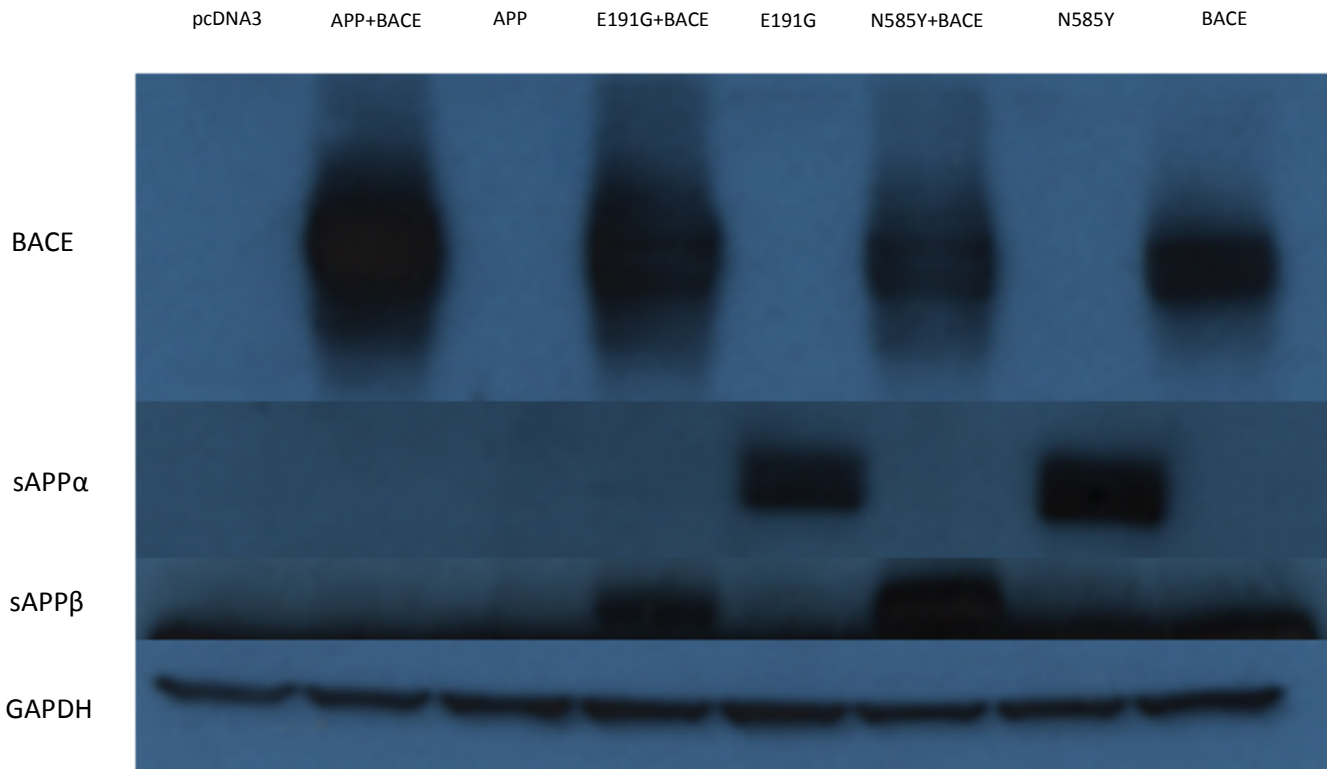

Figure 9. Western Blot for BACE, sAPPα, sAPPβ, and GAPDH in transfected CHO cells. BACE was only detected in samples transfected with the BACE pcDNA3 plasmid. Only cells transfected with mutant APP without BACE show sAPPα. The N585Y mutant shows a stronger sAPPα band than E191G. Only cells transfected with mutant APP and BACE show sAPPβ. The blot was cropped to exclude a nonspecific band below. The N585Y mutant shows a stronger sAPPβ band than E191G.

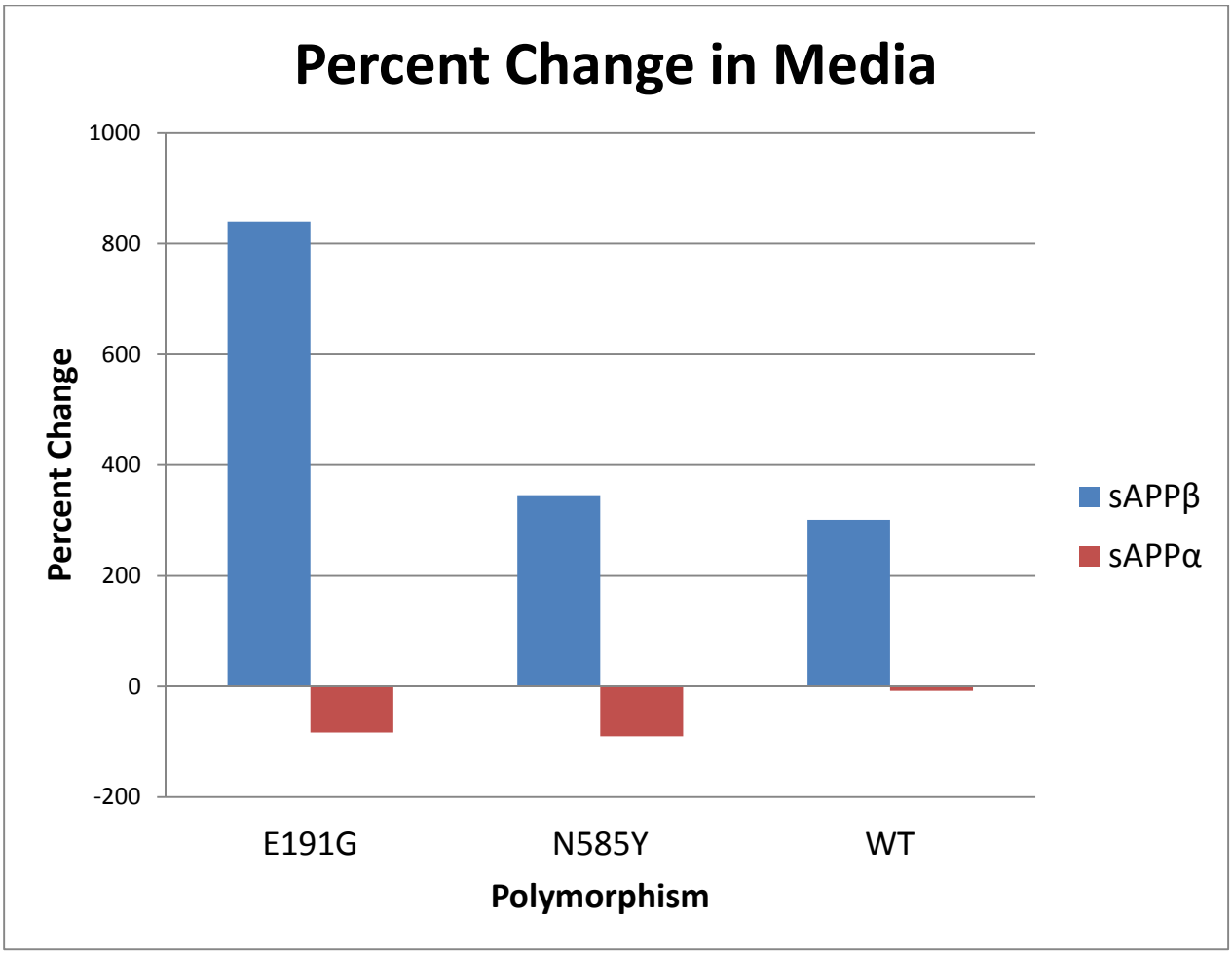

Figure 10. Percent change in the media after BACE transfection. The E191G mutant displayed the greatest change in sAPPβ levels.

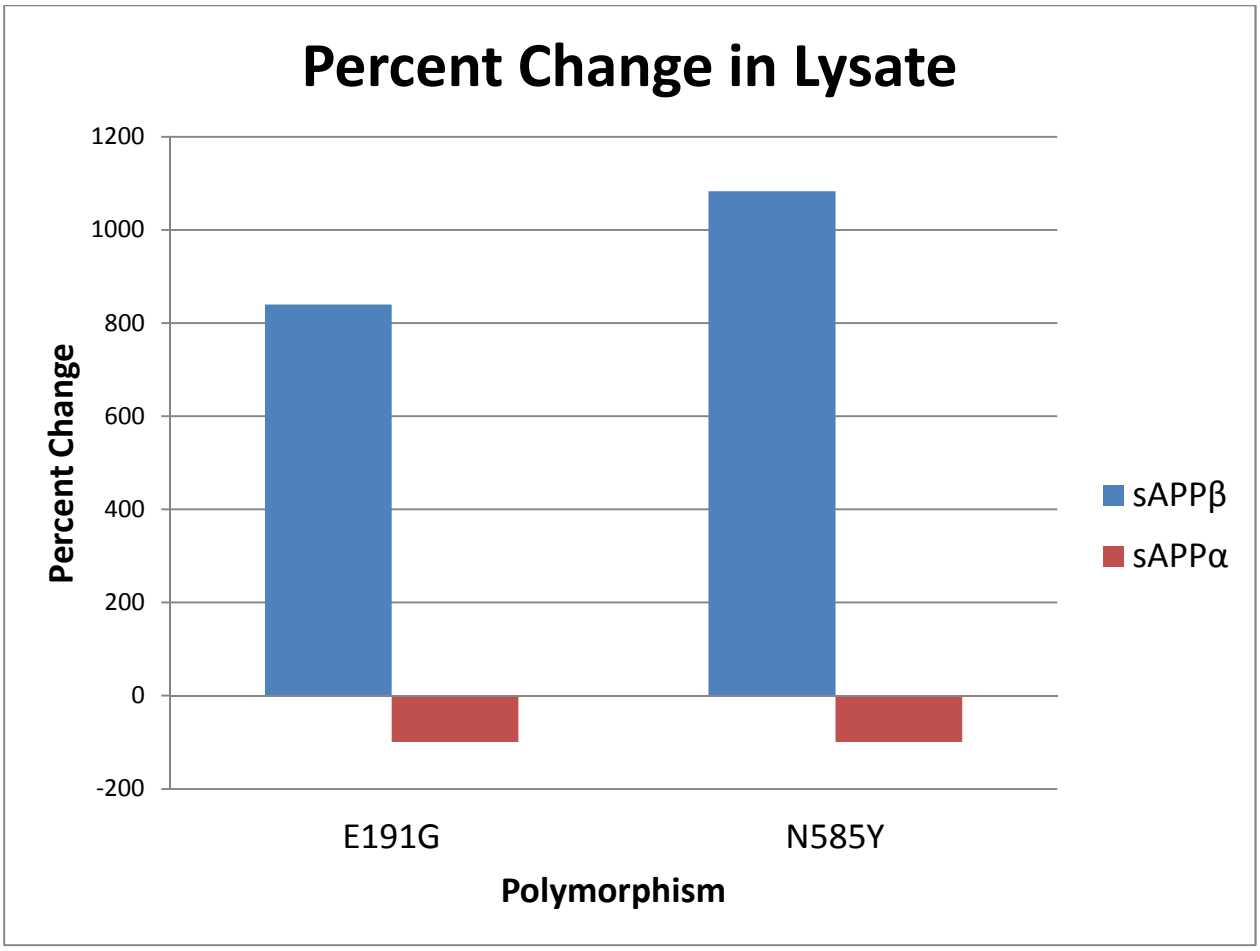

Figure 11. Percent change in the media of sAPPβ and sAPPα levels after BACE transfection. The N585Y displayed a greater change in sAPPβ levels.

IV. HEK293T Cells

To determine the effect of mutations on APP cleavage, mutant and wild-type APP was transfected into wild-type CHO cells. Cells were lysed after 24 hour incubation at 37^{o}C in 5% CO_2, and lysis was analyzed using a 4-12% bis-tris gel and western blot. Primary antibody 3E9 was used to detect the presence of mutant or wild-type APP mutants (figure 12). APP and APP mutants were successfully expressed in HEK cells. Untransfected HEK cells did not express any

APP. Following western blot, AlphaLISA assay was used to measure levels of Aβ and sAPPα. For this experiment we also used the H147N mutation along with the other two mutations described above. Results showed a significant decrease in the H147N levels of Aβ, suggesting this mutation could be protective against LOAD while the Aβ levels for N585Y and E191G mutants were unaffected (figure 13). The N585Y mutation showed a significant decrease in sAPPα levels, while the H147N and E191G mutations were unaffected (figure 14) suggesting that it has a greater propensity to be pathogenic. Using the data obtained from sAPPα and Aβ measurements, the ratio of sAPPα to Aβ was calculated (figure 15). The ratio of sAPPα/Aβ was decreased in cells transfected with N585Y. Cells transfected with E191G did not show an increase or decrease. The H147N showed a great increase in the ratio of sAPPα to Aβ.

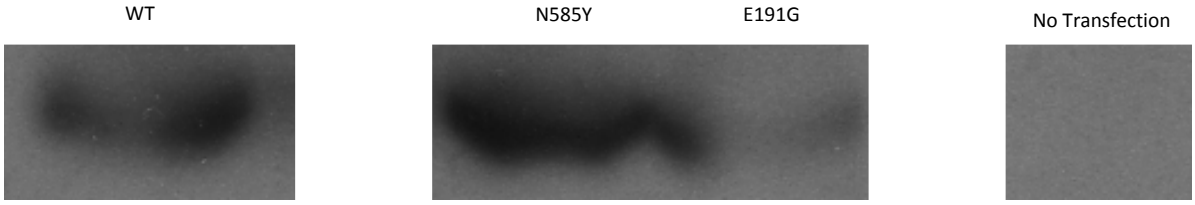

Figure 12. Western blot for APP in transfected HEK cells. No APP was detected in nontransfected samples and not a significant amount of E191G possibly due to proteolysis.

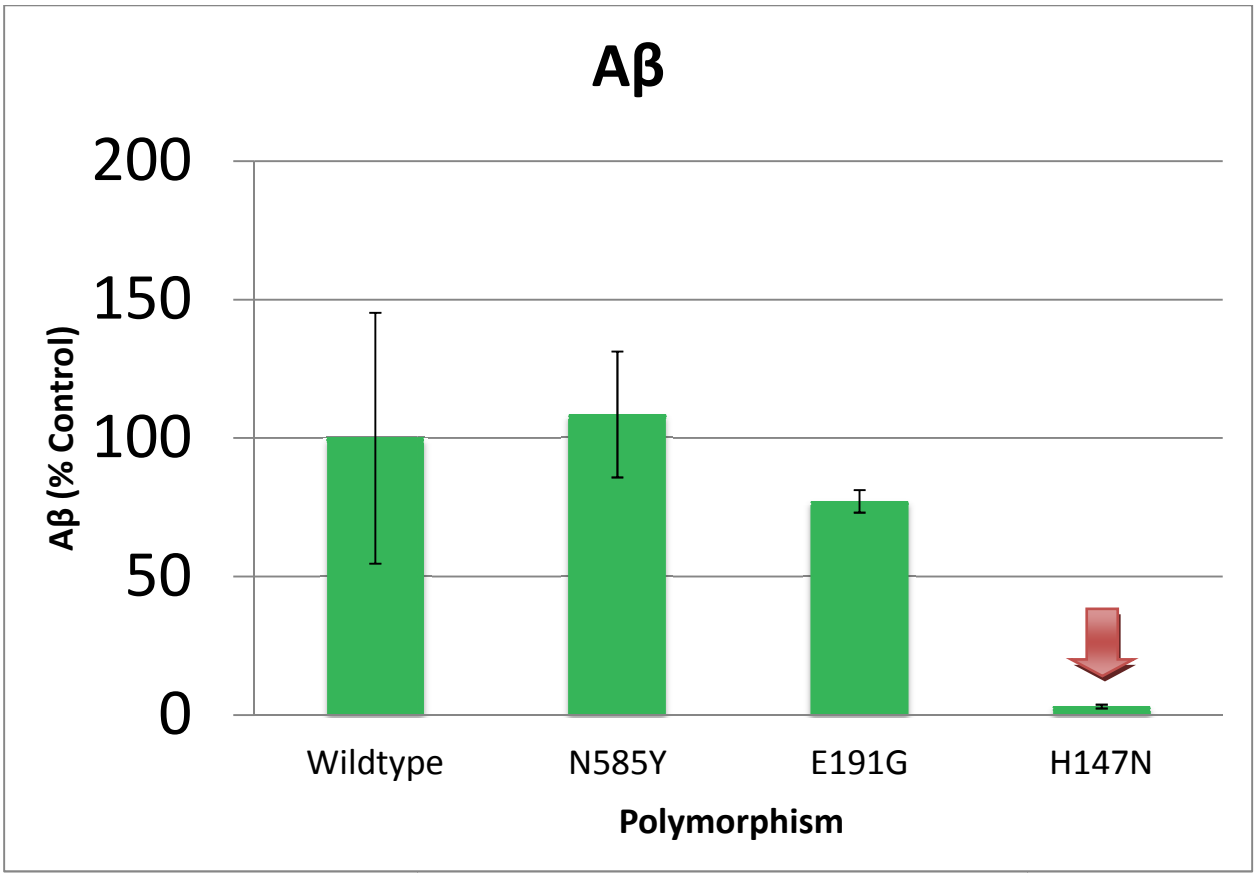

Figure 13. Aβ levels from transfected HEK cell lysate by AlphaLISA assay. H147N shows decreased Aβ production (arrow).

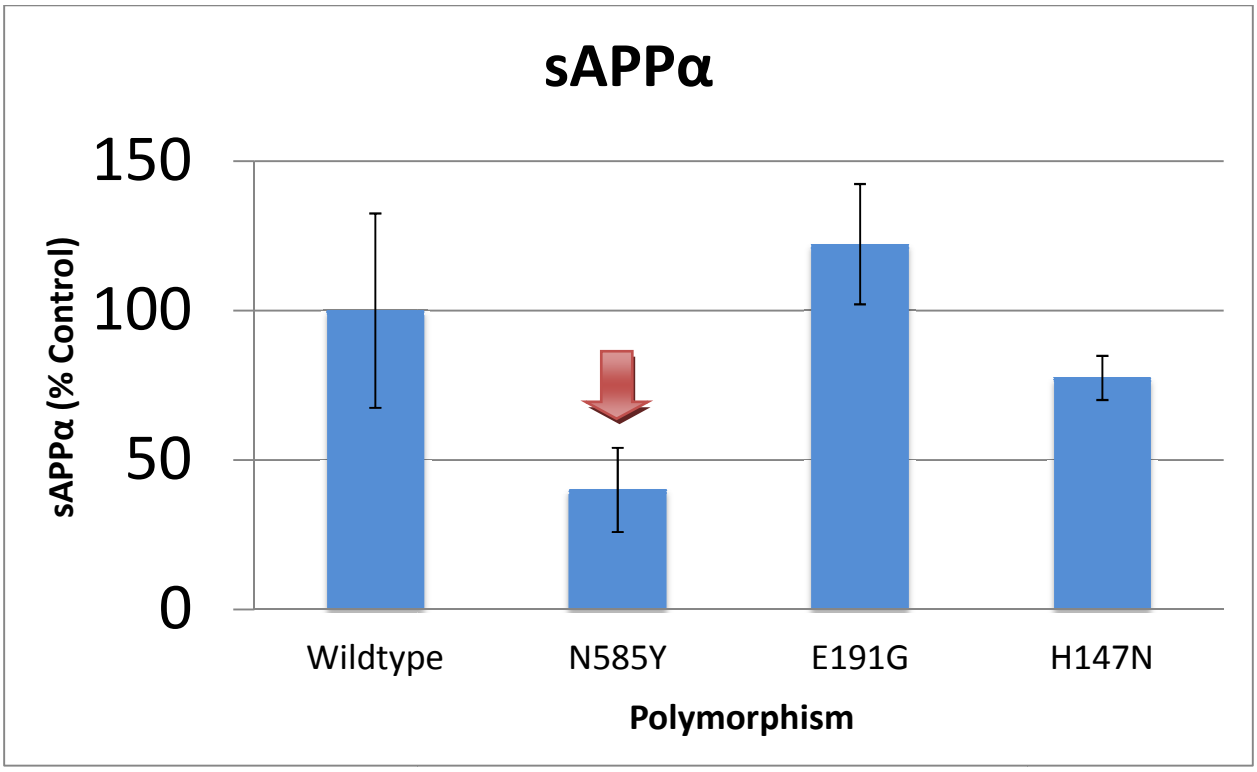

Figure 14. sAPPα levels from transfected HEK cells by AlphaLISA assay. The N585Y shows decreased sAPPα levels (arrow).

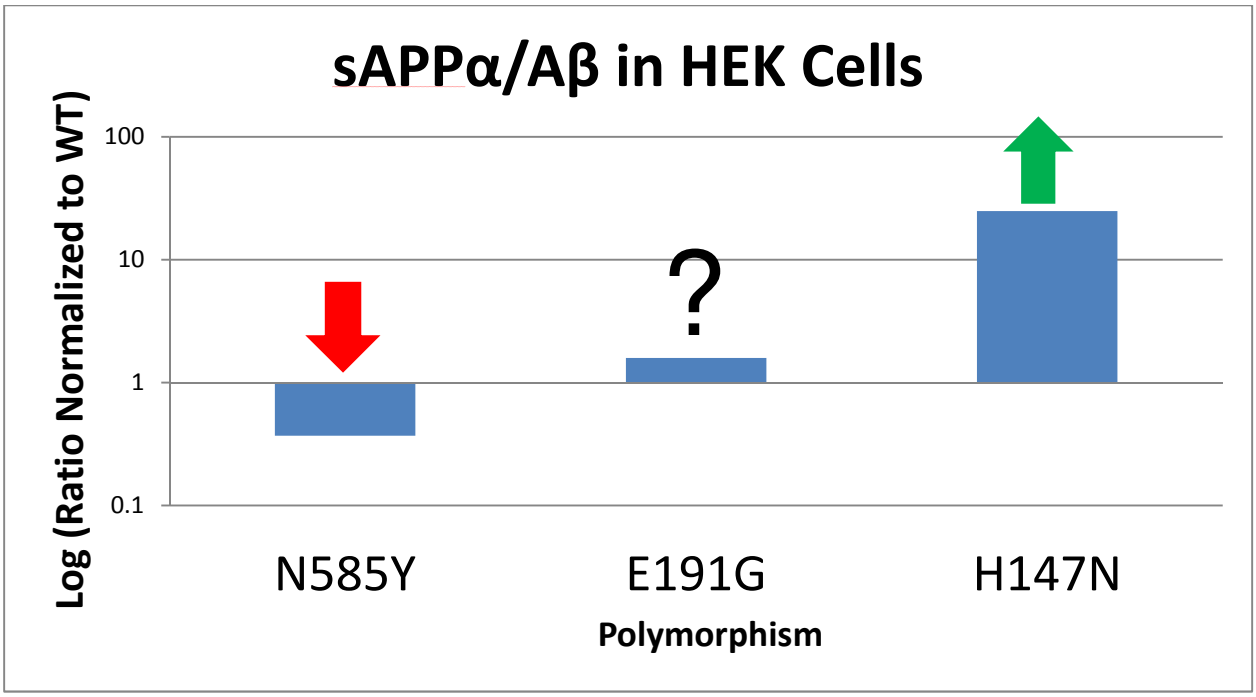

Figure 15. The log of the ratio of sAPPα to Aβ levels in HEK cell media normalized to wild-type ratio. The ratio of sAPPα/Aβ was decreased in the cells transfected with N585Y and increased in cells transfected with H147N. Cells transfected with E191G showed only slight variation from wild-type.

Discussion

Our results have shown that only the N585Y mutation can result in APP proteolysis leading to decreased trophic sAPPα and increased anti-trophic sAPPβ. The N585Y is located near the binding site of APP and BACE1. It is possible that the N585Y mutation alters the binding site of this complex, increasing the affinity between BACE1 and APP, resulting in increased proteolytic BACE1 activity and an increase in the production of anti-trophic factors in

individuals with the N585Y mutation. This increase in anti-trophic factor production in our experiments suggests that individuals with the N585Y mutation are at greater risk of LOAD.

The E191G mutation is located distal from the APP-BACE1 binding site in the acidic region of APP. While this mutation would not alter the binding site, it is possible that these mutations could change the conformation of the APP protein, affecting either BACE1 or ADAM10 binding leading to altered APP proteolysis. Results for the E191G mutation show that sAPPβ levels in the media of CHO cells showed a greater increase in BACE activity than the N585Y mutation (figure 10). However, the sAPPβ levels in cell lysate showed that the N585Y mutation produce greater amounts of anti-trophic peptides (figure 11) suggesting that the E191G mutation allows for better trafficking to and excretion through the plasma membrane.

In contrast, the H147N mutation in the CuBD has been previously reported to increase sAPPα, and in our experiments we show that it would confer a protective effect against LOAD.

BACE1 cleavage of APP results in the formation of sAPPβ. During the transition from APP to sAPPβ, a structural change occurs. It is possible that APP ectodomain mutations alter the structure of APP and affect APP proteolysis. For example, a mutation that decreases the stability of sAPPβ, while not affecting the stability of APP, would result in increased BACE1 cleavage. A mutation that increases the stability of sAPPβ, while not affecting the stability of APP, would result in decreased BACE1 cleavage.

Computer modeling (figure 7) has allowed us to form a hypothesis about some of the effects of LOAD mutations. Further investigation of these mutations will be necessary to

determine the accuracy of those predictions. Mutant APP695 will be transfected into CHO cells, and cleavage products will be measured and compared to cleavage products from wild-type APP695. Purified mutant APP695 will be tested using fluorescence and AlphaLISA assays.

Mutant and wild-type APP was transfected into CHO cells. Western blot results show that GAPDH levels appeared similar in all samples, indicating that the total protein levels in each well were equal. BACE was only detected only in samples where the BACE pcDNA3 plasmid had been transfected, showing that BACE transfections were successful and that BACE was not present in cells not transfected with BACE pcDNA3 plasmid. Western blots for sAPPα and sAPPβ showed sAPPα present only in mutant samples not transfected with BACE. Therefore, nontransfected CHO cells primarily cleave transfected mutant APP at the α-site. However in CHO cells also transfected with BACE, sAPPβ was detected in western blots rather than sAPPα. When CHO cells were transfected with BACE pcDNA3 plasmid, mutant APP was cleaved primarily at the β-site. Western blots for sAPPα and sAPPβ also showed that no cleavage products were detected for wild-type APP transfections, indicating an issue with the wild-type APP pcDNA3 plasmid. The wild-type plasmid is a necessary part of the experiment, and before further transfections can occur the wild-type APP pcDNA3 plasmid reagent should be quantified using nanodrop technology and possibly sequenced. If further issues occur, fresh wild-type APP pcDNA3 should be synthesized before continuing the project. Western blots using the 3E9 antibody for APP showed APP present in all samples, including those where APP was not transfected. This could mean that CHO cells express endogenous APP or that the pcDNA3 plasmid and BACE pcDNA3 contain APP. If CHO cells do express endogenous APP, a

different cell type would be better for our experiments. DNA sequencing should be used to determine if suspect plasmids contain APP.

CHO cell media and lysate from transfections were analyzed by ELISA assay. The first measurements were taken using a single set of samples from media collected after 24 and 48 hours of incubation and cells lysed after 48 hours of incubation. Measurements matched western blot results showing that sAPPα was only detected in cells transfected with only mutant APP. When BACE was present, sAPPα levels were low. Also matching western blot results, the N585Y mutant showed higher sAPPα levels than the E191G mutant. According to these results, the N585Y mutation may have a higher affinity for α secretase than the E191G mutation. When BACE was added, sAPPα levels dropped steeply for both mutants, with the E191G displaying higher sAPPα levels than the N585Y. In the future, the assay will have to be done with more samples to obtain standard deviations.

The ELISA assay measurements were taken using 3 sets of samples that were pooled together. Normally, it would be better to make measurements by measuring the 3 samples individually and calculating the average and standard deviation. However, we were short of reagents and opted to pool the samples together to obtain results that would be more accurate that measuring one sample alone. Results matched what we discovered from the western blots and first ELISA assay.

The third ELISA assay measurements were taken in the same way as the second measurements. Cells transfected with mutant APP and BACE showed high levels of sAPPβ compared to cells transfected with just mutant APP, matching western blot results. The N585Y

mutation produced greater levels of sAPPβ than the E191G mutation, indicating that it may have more affinity for BACE and could lead to increased pro-AD fragments.

Western blots of HEK293T cells showed that no endogenous APP was being expressed unlike CHO cells where some level of APP expression was observed. Hence, use of HEK293T cells for our experiments is better than CHO cells.

The AlphaLISA results obtained from HEK cell transfections showed that the H147N mutation displayed a decrease in Aβ levels and an increase in sAPPα/Aβ ratio, and the N585Y mutation displayed a decrease in sAPPα levels and a decrease in sAPPα/Aβ ratio (figure 16). The H147N mutation could possibly be protective against AD by lowering levels of Aβ in the brain. Identification of this mutation in human APP has not been reported. The data suggests that the H147 residue may play an important role in dictating a protective conformation of APP. The H147N mutation is located far from the Aβ region and β-site of APP. In order to affect Aβ production, the H147N mutant might disrupt the shape of APP, altering APP ability to interact with β-secretase. Another possibility is that the H147N mutation affects the copper binding domain, which is located nearby. The activity of the copper binding domain may play an unknown role in APP proteolysis that could be affected by mutation.

	sAPPα	Aβ	sAPPα/Aβ
WT	-	-	-
N585Y	↓	-	↓
E191G	-	-	↑
H147N	-	↓	↑

Figure 16. Table summarizing the results in HEK cells. The N585Y showed decreased levels of sAPPα and decreased ratio of sAPPα/Aβ. The E191G slightly increased the ratio of sAPPα/Aβ. Finally, the H147N decreased Aβ levels and increased the ratio of sAPPα/Aβ.

Conclusion

The N585Y mutation showed a decrease in sAPPα levels and an increase in sAPPβ in both CHO and HEK cells and decreased sAPPα/Aβ ratio, hence this mutation would increase the risk of onset of LOAD. Unlike the H147N mutation, which we show decreased Aβ and increased sAPPα/Aβ ratio and would be protective against LOAD, and the E191G mutation, which appears to be less harmful, the N585Y mutation is located near the α and β cleavage sites. The N585Y mutation appears to alter the ability of APP to interact with BACE or ADAM10, thus leading to a decrease in sAPPα levels. In the brain, lower levels of sAPPα would lead to a decreased trophic

effect on neurons. With less trophic factors, neural cells have decreased lifespan leading to quicker neurodegeneration. Individuals that have the N585Y mutation, that could be determined by a blood based genetic analysis, should make necessary lifestyle changes, such as using the metabolic enhancement for neurodegenerative diseases (MEND) approach (42), to delay AD, as our data suggest these subjects are at higher risk.

References

1. Hebert LE, Weuve J, Scherr PA, Evans DA. Alzheimer disease in the United States (2010–2050) estimated using the 2010 census. Neurology. 2013;80(19):1778-1783. doi:10.1212/WNL.0b013e31828726f5.

2. Alzheimer's Association, 2015 Alzheimer's Disease Facts and Figures, Alzheimer's & Dementia, Volume 10, Issue 2.

3. National Center for Health Statistics. Deaths: Final Data for 2013. National Vital Statistics Report. Volume 64, Number 2. Hyattsville, Md.; 2015. Available at: http://www.cdc.gov/nchs/data/nvsr/nvsr64/nvsr64_02.pdf. Accessed February 26, 2015.

4. Hebert LE, Beckett LA, Scherr PA, Evans DA. Annual incidence of Alzheimer disease in the United States projected to the years 2000 through 2050. Alzheimer Dis Assoc Disord 2001;15(4):169–73

5. Vincent GK, Velkof VA. The Next Four Decades: The Older Population in the United States: 2010 to 2050. Washington, D.C.: U.S. Census Bureau; 2010.

6. Cummings JL, Morstorf T, Zhong K. Alzheimer's disease drug-development pipeline: Few candidates, frequent failures. Alzheimer Res Therapy 2014;6:37.

7. Haass C, Lemere CA, Capell A, Citron M, Seubert P, Schenk D, Lannfelt L, Selkoe DJ. The Swedish Mutation Causes Early-onset Alzheimer's Disease by Beta-Secretase Cleavage Within the Secretory Pathway. Nat Med. 1995 Dec;1(12):1291-6.

8. Yi L, Wu T, Luo W, Zhou W, Wu J. A non-invasive, rapid method to genotype late-onset Alzheimer's disease-related apolipoprotein E gene polymorphisms.Neural Regeneration Research. 2014;9(1):69-75. doi:10.4103/1673-5374.125332.

9. Kline A. Apolipoprotein E, amyloid-ß clearance and therapeutic opportunities in Alzheimer's disease. Alzheimer's Research & Therapy. 2012;4(4):32. doi:10.1186/alzrt135.

10. Campion D, Dumanchin C, Hannequin D, et al. Early-onset autosomal dominant Alzheimer disease: prevalence, genetic heterogeneity, and mutation spectrum. American Journal of Human Genetics. 1999;65(3):664-670.

11. Flinn JM, Bozzelli PL, Adlard PA, Railey AM. Spatial memory deficits in a mouse model of late-onset Alzheimer's disease are caused by zinc supplementation and correlate with amyloid-beta levels. Frontiers in Aging Neuroscience. 2014;6:174. doi:10.3389/fnagi.2014.00174.

12. Roberson ED, Scearce-Levie K, Palop JJ, Yan F, Cheng IH, Wu T, Gerstein H, Yu GQ, Mucke L. Reducing Endogenous Tau Ameliorates Amyloid β –Induced Deficits in an Alzheimer's Disease Mouse Model. Science. 2007 May 4;316(5825):750-4.

13. Bohm C, Chen F, Sevalle J, et al. Current and future implications of basic and translational research on amyloid-β peptide production and removal pathways. Molecular and Cellular Neuroscience.

14. Abelein A, Graslund A, Danielsson J. Zinc as a Chaperone-mimicking agent for retardation of amyloid β peptide fibril formation. Proc Natl Acad Sci U S A. 2015 Mar 30. pii: 201421961.

15. DeToma AS, Krishnamoorthy J, Nam Y, Lee HJ, Brender JR, Kochi A, Lee D, Onnis V, Congiu C, Manfedini S, Vertuani S, Balboni G, Ramamoorthy A, Lim MH. Synthetic Flavenoids, Aminoisoflavones: Interaction and Reactivity with Metal-free and Metal-associated Amyloid-β Species. Chem Sci. 2014 Dec 1;5(12):4851-4862.

16. Shaked GM, Kummer MP, Lu DC, Galvan V, Bredesen DE, Koo EH. Aβ induces cell death by direct interaction with its cognate extracellular domain on APP (APP 597–624). The FASEB journal□: official publication of the Federation of American Societies for Experimental Biology. 2006;20(8):1254-1256. doi:10.1096/fj.05-5032fje.

17. Lu DC, Soriano S, Bredesen DE, Koo EH. Caspase Cleavage of the Amyloid Precursor Protein Modulates Amyloid-beta Toxicity. J Neurochem. 2003 Nov;87(3):733-41.

18. Kim T, Vidal GS, Djurisic M, et al. Human LilrB2 Is a β-Amyloid Receptor and Its Murine Homolog PirB Regulates Synaptic Plasticity in an Alzheimer's Model. Science (New York, NY). 2013;341(6152):10.1126/science.1242077. doi:10.1126/science.1242077.

19. Laurén J, Gimbel DA, Nygaard HB, Gilbert JW, Strittmatter SM. Cellular Prion Protein Mediates Impairment of Synaptic Plasticity by Amyloid-β Oligomers.Nature. 2009;457(7233):1128-1132. doi:10.1038/nature07761.

20. Decker H, Jurgensen S, Adrover MF, Brito-Moreira J, Bomfim TR, Klein WL, Epstein AL, De Felice FG, Jerusalinsky D, Ferreira ST. N-methyl-D-aspartate Receptors are Required for Synaptic Targeting of Alzheimer's Toxic Amyloid-β Peptide Oligomers. J Neurochem. 2010 Dec;115(6):1520-9. doi: 10.1111/j.1471-4159.2010.07058.x. Epub 2010 Nov 11.

21. Butterfield DA, Bush AI. Alzheimer's Amyloid Beta-Peptide(1-42): Involvement of Methionine Residue 35 in the Oxidative Stress and Neurotoxicity Properties of this Peptide. Neurobiol Aging. 2004 May-Jun;25(5):563-8.

22. Shahani N, Brandt R. Functions and Malcuntions of the Tau Proteins. Cell Mol Life Sci. 2002 Oct;59(10):1668-80.

23. Drewes G, Ebneth A, Preuss U, Mandelkow EM, Mandelkow E. MARK, a novel family of protein kinases that phosphorylate microtubule-associated proteins and Trigger Microtubule Disruption. Cell. 1997 Apr 18;89(2):297-308

24. Tepper K, Biernat J, Kumar S, et al. Oligomer Formation of Tau Protein Hyperphosphorylated in Cells. The Journal of Biological Chemistry. 2014;289(49):34389-34407. doi:10.1074/jbc.M114.611368.

25. Coburger I, Dahms SO, Roeser D, Gührs K-H, Hortschansky P, Than ME. Analysis of the Overall Structure of the Multi-Domain Amyloid Precursor Protein (APP). Yan R, ed. PLoS ONE. 2013;8(12):e81926. doi:10.1371/journal.pone.0081926.

26. Bredesen DE. Neurodegeneration in alzheimer's disease: Caspases and synthetic element interdependence. Molecular Neurodegeration. 2009;4(27).

27. Lourenço F, Galvan V, Fombonne J, et al. Netrin-1 interacts with amyloid precursor protein and regulates amyloid-β production. Cell death and differentiation. 2009;16(5):655-663. doi:10.1038/cdd.2008.191.

28. Lourenço F, Galvan V, Fombonne J, et al. Netrin-1 interacts with amyloid precursor protein and regulates amyloid-β production. Cell death and differentiation. 2009;16(5):655-663. doi:10.1038/cdd.2008.191.

29. Libeu CP, Poksay KS, John V, Bredesen DE. Structural and functional alterations in amyloid-β precursor protein induced by amyloid-β peptides. Journal of Alzheimer's Disease. 2011;25(3):547-566.

30. Miar A, Alvarez V, Corao AI, et al. Ayloid precursor protein gene (APP) variation in late-onset alzheimer's disease. Journal of Molecular Neuroscience. 2011;45:5-9.

31. Rice HC, Young-Pearce TL, Selkoe DJ. Systematic evaluation of candidate ligands regulating ectodomain shedding of amyloid precursor protein. Biochemistry. 2013;52(19):3264-3267.

32. Obregon D, Hou H, Deng J, et al.

sAPP-α modulates β-secretase activity and amyloid-β generation. Nat Commun. 2012;3.

33. Libeu C. P., Campagna J, Mitsumori M, Poksay K., Spilman P, Sabogal A, . . . John V.sAPPa is a potent endogenous inhibitor of BACE 1. Journal of Alzheimer's Diseae. 2015

34. Coburger I, Dahms SO, Roeser D, Gührs K-H, Hortschansky P, Than ME. Analysis of the Overall Structure of the Multi-Domain Amyloid Precursor Protein (APP). Yan R, ed. PLoS ONE. 2013;8(12):e81926. doi:10.1371/journal.pone.0081926.

35. Xu K, Olsen O, Tvetkova-Robev D, Tessier-Lavigne M, Nikolov DB. The Crystal Structure of DR6 in Complex With the Amyloid Precursor ProteinProvides Insight into Death Receptor Activation. Genes Dev. 2015 Apr 15;29(8):785-90. doi: 10.1101/gad.257675.114. Epub 2015 Apr 2.

36. Reinhard C, Hebert SS, De Strooper B. The amyloid-β precursor protein: Integrating structure with biological function. The EMBO Journal. 2005;24(23):3996-4006.

37. Haass C, Lemere CA, Capell A, Citron M, Seubert P, Schenk D, Lannfelt L, Selkoe DJ. The Swedish Mutation Causes Early-onset Alzheimer's Disease by Beta-Secretase Cleavage Within the Secretory Pathway. Nat Med. 1995 Dec;1(12):1291-6.

38. Murrell J, Farlow M, Ghetti B, Benson MD. A Mutation in the Amyloid Precursor Protein Associated With Hereditary Alzheimer's Disease. Science. 1991 Oct 4;254(5028):97-9.

39. Jonsson T, Atwal JK, Steinberg S, Snaedal J, Jonsson PV, Bjornsson S, Stefansson H, Sulem P, Gudbjartsson D, Maloney J, Hoyte K, Gustafson A, Liu Y, Lu Y, Bhangale T, Graham RR, Huttenlocher J, Bjornsdottir G, Andreassen OA, Jonsson EG, Palotie A, Behrens TW, Magnusson OT, Kong A, Thorsteinsdottir U, Watts RJ, Stefansson K. A Mutation in APP Protects Against Alzheimer's Disease and Age-Related Cognitive Decline. Nature. 2012 Aug 2;488(7409):96-9. doi: 10.1038/nature11283.

40. Cruchaga C, Chakraverty S, Mayo K, et al. Rare variants in APP,PSEN1, and PSEN2 increase risk for AD in late-ONset alzheimer's disease families. PLoS ONE. 2012;7(2).

41. Spoerri L, Vella LJ, Pham CLL, Barnham KJ, Cappai R. Amyloid precursor protein copper binding domain histidine residues 149 and 151 mediate APP stability and metabolism. The Journal of Biological Chemistry. 2012;287(32):26840-26853.

42. Bredesen DE. Reversal of cognitive decline: A novel therapeutic program. Aging (Albany NY). 2014;6(9):707-717.